

# Integrated Electro-optic Wavelength Filter With Programmable Spectral Response

H. Herrmann, D. Büchter, R. Ricken, and W. Sohler

Angewandte Physik, Universität Paderborn, Warburger Str. 100, 33098 Paderborn, Germany,  
e-mail: h.herrmann@physik.uni-paderborn.de

**Abstract:** An integrated optical circuit in  $\text{LiNbO}_3$  consisting of a sequence of electro-optic polarization converters is operated as wavelength filter with a programmable spectral response. Bandpass filter operation with strong sidelobe suppression, with flat-top filter response and tuneability are demonstrated.

## Introduction

Wavelength filters are key components for many applications in optical communications and instrumentation with different demands on the filter characteristics. For instance, some applications require band pass characteristics with strong suppressions of sidelobes, others require tuneability and/or an especially tailored spectral response.

In recent years several types of integrated optical filters have been demonstrated. Among them are integrated electro-optic filters in  $\text{LiNbO}_3$  which take advantage of the wavelength-selective polarization conversion induced by a periodic electric field [1,2]. These filters use a constant voltage applied to all converter electrodes and, hence, have a fixed sinc<sup>2</sup>-like spectral filter response. In this contribution we demonstrate for the first time a new mode of operation of such a filter which allows to obtain a programmable spectral response. The filter consists of a series of electro-optic polarization converters which enable to tailor the spectral response by individually addressing the different electrodes. Such a device has already been used for polarization mode dispersion compensation [3,4].

## Device structure and principle of operation

In a Ti-indiffused optical waveguide in X-cut, Y-propagating  $\text{LiNbO}_3$  a periodic electric field parallel to the Y-axis can induce a polarisation conversion, i.e. a coupling between TE- and TM-polarized modes via the  $r_{51}$  component of the electrooptic tensor [1]. This coupling along the propagation direction  $z$  can be described using the coupled-mode theory with amplitudes  $A_{TE}$  and  $A_{TM}$  of the TE- and TM-polarized modes:

$$\begin{aligned} \frac{\partial A_{TE}}{\partial z} &= i\kappa A_{TM} \exp(-i\Delta\beta z) \\ \frac{\partial A_{TM}}{\partial z} &= i\kappa A_{TE} \exp(+i\Delta\beta z) \end{aligned} \quad (1)$$

with  $\Delta\beta = \beta_{TM} - \beta_{TE} - 2\pi/\Lambda$ .  $\beta_{TE}$  and  $\beta_{TM}$  are the wave numbers of the TE- and TM-polarized modes, respectively.  $\kappa$  is the coupling coefficient depending on the applied voltage  $U$  and  $\Lambda$  is the periodicity of the electrode pattern.

An efficient conversion requires phase-matching and therefore  $\Delta\beta \approx 0$ , i.e. the difference of the wave numbers of the TE- and TM polarized modes must be compensated by the periodicity of the electric field. The period of the comb-like electrode pattern (Fig. 1) on top of the waveguide determines the wavelength at which phase-matching is fulfilled.

If the coupling strength along the interaction is constant, the spectral response is given by a sinc<sup>2</sup>-like function; it is approximately given by the square of the Fourier transform of the position dependent coupling coefficient  $\kappa(z)$ . This means that via a proper design of the coupling strength a tailoring of the spectral characteristics is possible. Similar schemes for tailoring a spectral response have already been demonstrated for instance to design integrated acoustooptical filters [5,6] or Bragg-type reflectors [7].

The idea of this work is to realize a programmable spectral response by using a sequence of electrode sections which can be individually addressed with different voltages. To have full freedom in the design of  $\kappa(z)$ , each electrode section consists of in-phase and quadrature interdigital electrodes, i.e. a section contains two interleaved electrodes with finger pairs which are shifted by a quarter of a period. One side is always grounded. The detailed structure of an electrode section is plotted in Fig. 2. A section is about 1.2mm long. In-phase and quadrature interdigital electrodes alternate after 6 or 7 finger pairs.

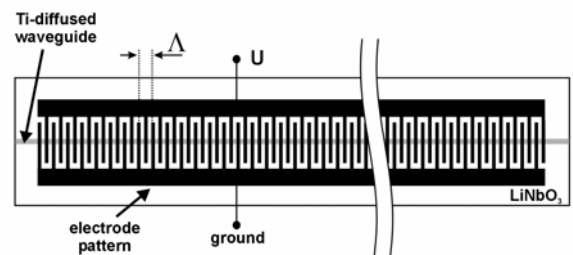


**Fig. 1:** Electrooptic polarisation converter with homogeneous coupling.

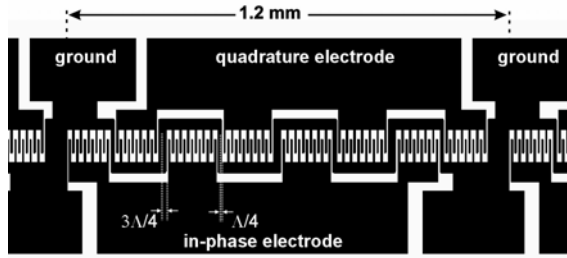


Fig. 2: Details of an electrode section with in-phase and quadrature electrodes.

The overall device consisting of  $N$  electrode sections is driven by the voltages  $U_{i1} \dots U_{iN}$  and  $U_{q1} \dots U_{qN}$  applied to the in-phase and quadrature electrodes, respectively.

### Modelling

For a given spatial dependence of the coupling coefficient the coupled-mode equations (1) must be solved to calculate the spectral response. They can be solved analytically for homogenous coupling. From this result a Jones matrix can be determined [1]. Each electrode section of the filter can be treated as an electro-optic converter with homogeneous coupling. The in-phase and the quadrature parts are taken into account by assuming an effective drive voltage  $U_{eff} = \sqrt{U_i^2 + U_q^2}$  and an additional relative phase-shift  $\Phi = \arctan(U_q/U_i)$  of the coupling strength with  $U_i$  and  $U_q$  being the in-phase and the quadrature drive voltages. The spectral response of the overall device can be calculated from the product of the Jones matrices of each section.

To obtain a desired spectral response the corresponding coupling strength function  $\kappa(z)$  must be determined and this function has to be discretized in order to find a proper set of voltages to be applied to the electrode sections. For a given spectral response  $\kappa(z)$  can be determined using an inverse scattering formalism [8]. However, this method is rather difficult. Therefore, we used the reverse way and started with trial functions for the coupling strength and optimized them until we achieved the desired result.

One example is the development of a filter with strong sidelobe suppression. We used some well-known window functions [7] for the shape of the coupling strength. In Fig. 3 the calculated spectral response is shown for a Kaiser-type window function [7] discretized into 20 sections (see also Fig. 7). For comparison, the spectral response for homogenous coupling is shown as well with sidelobes of about -10 dB below the maximum transmission. In contrast, a coupling strength which approximates a Kaiser-type window function leads to a filter response with sidelobe suppression better than 40 dB.

Wavelength tuning of the filter is possible if a phase-shift of the coupling strength between subsequent sections of the filters is imposed [1]. With such an additional phase-shift the wavelength of maximum conversion is shifted. This tuning can be realized by

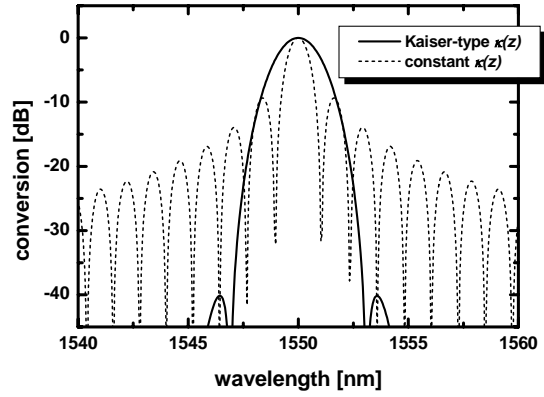


Fig. 3: Calculated spectral responses assuming a coupling strength function according to a Kaiser type window function discretized into 20 sections. For comparison the dashed line shows the response assuming a homogeneous coupling strength.

a proper adjustment of the in-phase and quadrature voltages. In Fig. 4 calculated spectral responses are shown assuming a Kaiser-type window function discretized to 16 sections for various relative phase shifts between subsequent sections. With increasing phase-shift satellite peaks occur which are about 25 nm separated from the central peak. This separation increases with shorter length of the electrode sections. However, within a spectral range of about 10 nm the filter can be tuned without getting satellite peaks of more than -10 dB height.

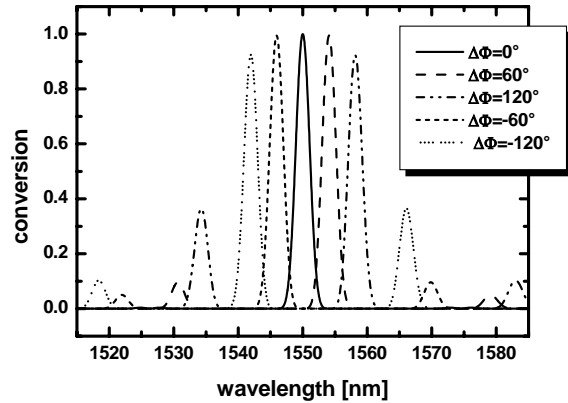


Fig. 4: Calculated tuning characteristics of a filter with 16 sections (Kaiser-type window). Between subsequent sections a relative phase-shift of  $\Delta\phi$  is imposed.

### Sample fabrication

Optical waveguides were fabricated by an indiffusion of 7  $\mu\text{m}$  wide and 100 nm thick Ti-strips into X-cut  $\text{LiNbO}_3$ . The diffusion was performed at 1060°C for 9h. Prior to the electrode fabrication an about 500 nm thick  $\text{SiO}_2$  buffer layer was deposited on the surface. Subsequently, about 500 nm thick gold electrodes according to the structure shown in Fig. 2 were evaporated. The overall sample has a length of 50 mm with 30 electrode sections; their period is  $\Lambda = 21.7 \mu\text{m}$ . To suppress spurious reflections at the



Fig. 5: Photograph of the sample.

end faces an AR-coating for the 1.55  $\mu\text{m}$  spectral region was deposited directly on the end faces.

Investigation of the waveguides in the spectral range around 1.55  $\mu\text{m}$  revealed that they are monomode and the losses are 0.1 dB/cm (TM polarization) and 0.4 dB/cm (TE), respectively.

Fig. 5 shows a photograph of the sample. It is mounted on a temperature stabilized copper holder in order to control the temperature during operation with about 0.1°C accuracy. The electrodes are contacted with thin wires to small strips of a printed circuit board beside of the sample.

### Experimental results

In the optical setup the amplified spontaneous emission from an Erbium-doped fiber amplifier is used as light source. The sample is mounted between crossed (external) polarizers. Butt-coupling using lenses with 10 mm focal length is used at the input and output sides of the sample. The transmitted light behind the rear polarizer is fed to an optical spectrum analyser with 0.1 nm resolution.

A computer controlled programmable voltage supply with up to 32 channels delivering -50V... +50V was used to drive the electro-optic converter sections.

In a first experiment a constant voltage of 11.2 V was applied to the in-phase electrodes of 20 sections. This gives rise to a complete conversion at the phase-match wavelength of 1553.4 nm. The corresponding measured spectral response is shown in Fig. 6. Due to inhomogeneities of the waveguide structure the shape of the spectral characteristics differs from the ideally expected  $\text{sinc}^2$ -function which is also plotted in the diagram. The spectral bandwidth of the measured curve is 1.1 nm and the largest sidelobe is 7.9 dB below the maximum transmission.

In order to suppress the sidelobes, the voltages applied to the in-phase electrodes were modified to approximate a Kaiser-type window function. In the upper diagram of Fig. 7 the corresponding voltages applied to the 20 electrodes are shown. The lower diagram presents the resulting measured and calculated spectral responses. It can be seen that the sidelobes are now strongly suppressed. The largest sidelobe of the measured characteristic is about 20.3 dB below the maximum transmission. On the other hand, the spectral 3dB-band width increases to 2.3

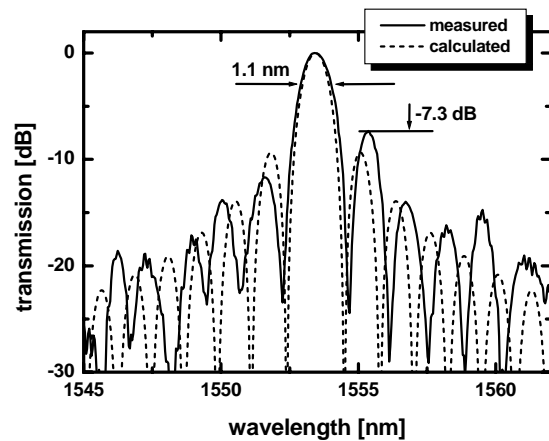


Fig. 6: Measured (solid line) and calculated (dashed line) spectral response of the filter with homogenous coupling.

nm.

Tuning of the filter as discussed in the section on modelling could be verified as well. We operated the device with 16 sections. In Fig. 8 the measured filter characteristics are shown for various relative phase shifts between subsequent sections. It can be seen that the filter is tunable as predicted from the theoretical results.

Another example of a tailored spectral response obtained with the programmable filter is shown in Fig. 9. The device has been programmed to give a (nearly) rectangular response, i.e. a flat-top characteristic. The corresponding coupling strength approximates a seventh-order Butterworth function. Due to

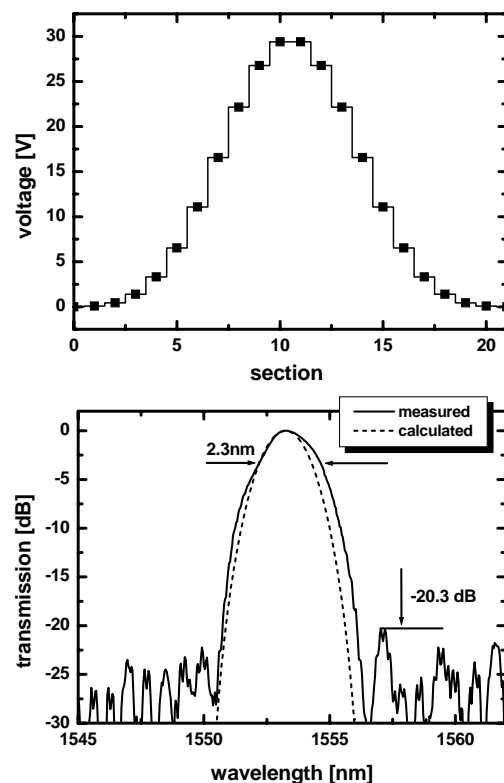
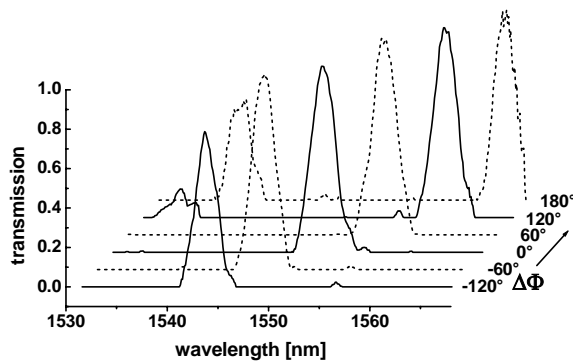
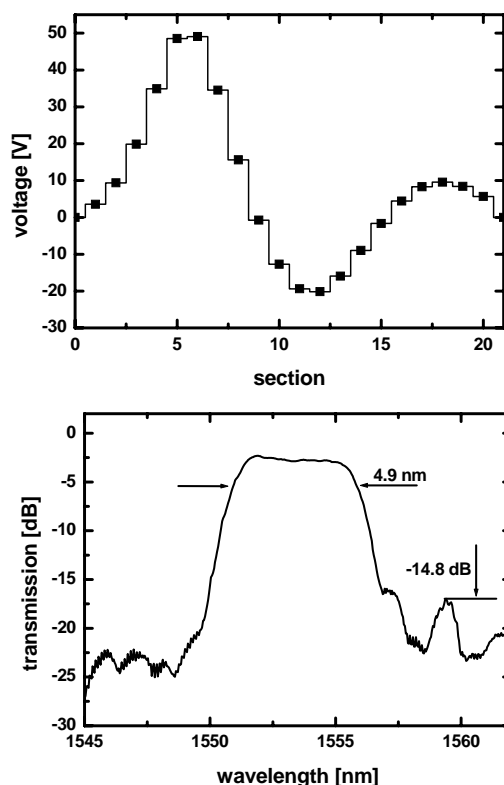


Fig. 7: Filter with strong sidelobe suppression. Voltages applied to the in-phase electrodes of the 20 sections (top diagram) and measured and calculated corresponding spectral responses.



**Fig. 8:** Measured tuning characteristics of a 16 sections filter with Kaiser-type coupling strength. The different curves are obtained by imposing a phase-shift of  $\Delta\Phi$  between subsequent sections.

the limited voltages available from our signal source, we could not obtain complete conversion. Maximum conversion is about  $-2.9$  dB. The spectral 3dB-width is about  $4.3$  nm and the highest sidelobe  $14.8$  dB below the maximum conversion.



**Fig. 9:** Flat-top operation of the filter: Voltages applied to the in-phase electrodes of the 20 sections (top diagram) and measured corresponding spectral response.

## Conclusions

We have demonstrated for the first time an integrated electrooptic wavelength filter with a programmable spectral response. Bandpass filter characteristics with high sidelobe suppression and flat-top response have been experimentally demonstrated as well as tunability of the filter. The results are in good agreement

with theoretically predicted results.

Further work will concentrate on the improvement of the filter performance. Of particular interest will be a polarization independent operation. This might be achieved by using a polarization diversity scheme. Furthermore, the integration of polarizers or polarization splitters (for the polarization independent device) to form a complete integrated optical circuit would be of great importance.

## References

- 1 F. Heismann, R. Alferness, *IEEE J. Quantum Electron.* QE-24, pp. 83-93 (1988)
- 2 W. Warzanskyj et al. *Appl. Phys. Lett.* vol. 53, pp. 13-15 (1988)
- 3 R. Noé et al., *Electronics Letters*, vol.35, pp.652-4 (1999)
- 4 R. Noé et al., *J. Sel. Top. Quantum Electron.*, vol. 10, pp. 341-355 (2004)
- 5 H. Herrmann et al., *J. Lightwave Technol.*, vol. 13, pp. 364-374 (1995)
- 6 D.A. Smith, J.J. Johnson, *APL*, vol. 61, pp.1025-1027 (1992)
- 7 P.S. Cross, H. Kogelnik, *Opt. Lett.* vol. 1, pp. 43-45 (1977)
- 8 G.-H. Song, S.-Y. Shin, *J. Opt. Soc. Am. A*, vol. 2, pp. 1905-1915 (1985)